Vietnam Journal of Science and Technology
DOI: https://doi.org/10.15625/2525-2518/21258

Assessment of some properties, morphology and film-forming ability of polycaprolactone/xanthan gum/chrysophanol composites

Nguyen Thuy Chinh[1,2], Trinh Hoang Nghia[3], Pham Thi Huyen[4], Thai Hoang[1,2,*]

[1]*Institute for Materials Science, Vietnam Academy of Science and Technology, 18 Hoang Quoc Viet street, Nghia Do ward, Ha Noi, 100000, Viet Nam*
[2]*Graduate University of Science and Technology, Vietnam Academy of Science and Technology, 18 Hoang Quoc Viet street, Nghia Do ward, Ha Noi, 100000, Viet Nam*
[3]*Université du Québec à Trois - Rivières, 3351 Boulevard des Forges, Trois – Rivières, Québec, Canada*
[4]*Hanoi University of Industry, 298 Cau Dien street, Tay Tuu ward, Ha Noi, 100000, Viet Nam*

[*]Email: *hoangth@itt.vast.vn*

Received: 31 July 2024; Accepted for publication: 30 September 2024

Abstract. This study presents the effect of some auxiliary agents (polyethylene oxide (PEO), polyethylene glycol (PEG), Tween 80, and Tween 20) on the film-forming ability, properties, and morphology of the PCL/XG/CSP composites. The composite films were prepared by the solution casting method, in which PCL and CSP were dissolved in dichloromethane and XG was dissolved in distilled water. The emulsifiers such as PEG, Tween 80, and Tween 20 in liquid form were added to the PCL/CSP solution while PEO in powdery form was dissolved together with XG in distilled water. From the obtained results, the PCL/XG/CSP composites cannot form a film in the case of the addition of PEG, Tween 80, and Tween 20 while using PEO, even and smooth composite films were obtained. The processing conditions consisting of PEO content, PCL/XG ratio, and PCL and XG concentration in solution were also investigated to assess their influence on the morphology, structure, and mechanical properties of the PCL/XG/CSP/PEO composite films. With the highest tensile strength and elongation at break, the most uniform structure, the PCL/XG/CSP/PEO composite film prepared with the PEO content of 0.6 g, the PCL content of 0.14 g, the XG content of 0.06 g are the best sample among tested ones. The other characteristics including thermal property, crystal property, and surface property of the composite film prepared at the most suitable conditions have been also assessed.

Keywords: biocomposite film, solution casting method, emulsifiers, morphology.

Classification numbers: 2.3.1, 2.7.1.

1. INTRODUCTION

In recent years, the research on biodegradable biomaterials based on natural and synthetic polymers has garnered significant attention from scientists due to their exceptional properties, such as high biocompatibility, deep cell adhesion, non-toxicity, and rapid biodegradation, etc. [1-3]. Various fabrication methods for biomaterials exist [4-7], among them, the solution method

is particularly popular for synthesizing biomedical polymers owing to its simplicity, minimal equipment requirements, and quick prototyping time [8]. Typically, polymers and bioactive compounds are dissolved in suitable solvents before being combined. This method produces films with high uniformity in thickness and clarity, devoid of cracks while exhibiting good mechanical properties, making them suitable for laboratory and industrial applications [9, 10].

Polycaprolactone (PCL), a biodegradable polymer has extensive applications in scientific and industrial fields, particularly in biomedicine due to its excellent biocompatibility, drug delivery capabilities, non-toxicity, biodegradability, and remarkable flexibility [11-14]. The PCL has been approved by the FDA for drug delivery systems and absorbable sutures [13]. However, some limitations of PCL include poor film-forming properties and lower mechanical strength, alongside slower degradation rates compared to natural polymers [15]. To overcome its disadvantages, it can be combined PCL with xanthan gum (XG), a natural polymer that improves drug solubility and absorption to enhance these qualities. The XG, known for its ability to interact with various polymers and proteins, contributes to the stability of the formed materials against degrading enzymes while increasing the solubility of hydrophobic drugs [16, 17].

This study utilizes chrysophanol (CSP), a bioactive compound with numerous biological activities, as a model drug, offering potential therapeutic benefits such as antiviral, anti-inflammatory, antioxidant, and anticancer properties [18-20]. Due to the inherent differences in the properties of PCL (hydrophobic polymer) and XG (hydrophilic polymer), their compatibility and blending present significant challenges. Additionally, the CSP is a substance characterized by high hydrophobicity and poor solubility in water, making its uniform dispersion within the PCL/XG matrix particularly difficult. Therefore, the incorporation of compatibilizers, referred to as emulsifiers, is essential for the effective mixing of XG, PCL, and CSP. Common compatibilizers such as Tween 80, Tween 20, polyethylene oxide (PEO), and polyethylene glycol (PEG), play a crucial role in this process [7]. Moreover, the PEO and PEG can be also considered as film-forming agents when they are combined with other polymers [21-23]. In our previous study, the PCL/XG/CSP composites were prepared in powder form using sodium tripolyphosphate as a cross-linking agent and the Tween 20 and PEO as compatibilizers [24]. With the excellent bioactivities of CSP, the PCL/XG/CSP composites in the film form have the potential for application as stickers in the treatment of wound healing or food packaging. Thus, this work focuses on investigating the effects of some auxiliary agents consisting of Tween 80, Tween 20, PEO, and PEG on the structure, morphology, and film-forming ability of the PCL/XG/CSP composite materials prepared via the solution casting method. Moreover, some other characteristics including thermal properties, crystal structure, and water contact angle of the composite films prepared at the most suitable conditions have also been assessed and discussed.

2. MATERIALS AND METHODS

2.1. Materials

The chemicals used in this study include polycaprolactone (PCL, an average $M_n \sim 10000$), xanthan gum from *Xanthomonas campestris* (XG, a viscosity of 800-1200 cps), chrysophanol (CSP, 98 %), polyethylene oxide (PEO, 99 %, an average $M_v \sim 100000$), polyethylene glycol (PEG, an average M_n 400), Tween 20 (polyoxyethylene (20) sorbitan monolaurate, a concentration ≥ 40.0 %), Tween 80 (polyoxyethylene (20) sorbitan monooleate, oleic acid ≥ 58.0 %), dichloromethane (DCM, ≥ 99.5 %). All were provided by Sigmal Aldrich.

2.2. Preparation of PCL/XG/CSP composites

In this study, the ratio of PCL/XG in the composites as well as the amount of some auxiliary agents would be assessed. The composition of components in the composites is presented in Table 1. The procedure for preparing PCL/XG/CSP composite films is presented as follows: Firstly, the XG was dissolved in 10 mL of distilled water for 30 minutes at 50 °C (solution A). At the same time, the PCL was dissolved in 2 mL of DCM at room temperature, following adding CSP to form solution B. Next, the PEG, Tween 80, or Tween 20 were added to solution B while PEO was added to solution A. The mixture was stirred on a magnetic stirrer for 30 minutes and vortexed for 5 minutes. Then solution B was added slowly to solution A before the mixture was stirred for 30 minutes at 50 °C. The mixture was then ultrasonicated for 30 minutes at 30 °C and magnetically stirred for 1 hour at 50 °C. After that, the final mixture was poured into a Petri dish and let natural solvent evaporation to obtain PCL/XG/CSP composite films. Table 1 shows the composition and signature of the tested samples. The samples from No. 1 to No. 20 are samples containing one of PEO, PEG, Tween 80, or Tween 20, from No. 21 to No. 24 are samples with the change of PEO weight, and from No. 25 to No. 27 are samples with the change of PCL and XG weight in solutions A and B.

Table 1. The composition and signature of the PCL/XG/CSP composite films.

No.	Abbreviation	XG (g)	PCL (g)	CSP (g)	PEO (g)	PEG (g)	Tween 80 (g)	Tween 20 (g)
1	XPC46	0.04	0.06	0.0005	0	0	0	0
2	XPC46PEO6	0.04	0.06	0.0005	0.6	0	0	0
3	XPC46PEG6	0.04	0.06	0.0005	0	0.6	0	0
4	XPC46Tween806	0.04	0.06	0.0005	0	0	0.6	0
5	XPC46Tween206	0.04	0.06	0.0005	0	0	0	0.6
6	XPC37	0.03	0.07	0.0005	0	0	0	0
7	XPC37PEO6	0.03	0.07	0.0005	0.6	0	0	0
8	XPC37PEG6	0.03	0.07	0.0005	0	0.6	0	0
9	XPC37Tween806	0.03	0.07	0.0005	0	0	0.6	0
10	XPC37Tween206	0.03	0.07	0.0005	0	0	0	0.6
11	XPC28	0.02	0.08	0.0005	0	0	0	0
12	XPC28PEO6	0.02	0.08	0.0005	0.6	0	0	0
13	XPC28PEG6	0.02	0.08	0.0005	0	0.6	0	0
14	XPC28Tween806	0.02	0.08	0.0005	0	0	0.6	0
15	XPC28Tween206	0.02	0.08	0.0005	0	0	0	0.6
16	XPC19	0.01	0.09	0.0005	0	0	0	0
17	XPC19PEO6	0.01	0.09	0.0005	0.6	0	0	0
18	XPC19PEG6	0.01	0.09	0.0005	0	0.6	0	0
19	XPC19Tween806	0.01	0.09	0.0005	0	0	0.6	0
20	XPC19Tween206	0.01	0.09	0.0005	0	0	0	0.6
21	XPC37PEO4	0.03	0.07	0.0005	0.4	0	0	0
22	XPC37PEO2	0.03	0.07	0.0005	0.2	0	0	0
23	XPC37PEO1	0.03	0.07	0.0005	0.1	0	0	0
24	XPC37PEO0.5	0.03	0.07	0.0005	0.05	0	0	0
25	XPC614PEO6	0.06	0.14	0.0010	0.6	0	0	0
26	XPC921PEO6	0.09	0.21	0.0015	0.6	0	0	0
27	XPC1228PEO6	0.12	0.28	0.0020	0.6	0	0	0

2.3. Characterization

The structure of PCL/XG/CSP composite films has been evaluated by Fourier transform infrared (FT – IR) using a Nicolet iS10 (USA) with the conditions: a resolution of 8 cm^{-1}, scans of 16 times, and at room temperature. The morphology of PCL/XG/CSP composite films has been assessed using a SZ61 stereo microscope (Olympus, Japan). The tensile strength and elongation at break of PCL/XG/CSP composite films were tested according to ASTM D882 standard on a Zwick testing machine (Germany). The scanning electron microscopy (SEM) images of the samples were taken on a FESEM4800 (Hitachi, Japan). Differential scanning calorimetry (DSC) analysis of the samples was carried out using a DSC204F1 (Netzsch, Germany) in the conditions: heating rate of 10 °C/minute, from room temperature to 350 °C in a nitrogen atmosphere. The water contact angle (WCA) of the samples was determined on an OCA50 device (Dataphysics, Germany). X-ray diffraction (XRD) analysis of the samples was taken on a Commander device with CuKα of 1.54 nm.

3. RESULTS AND DISCUSSION

3.1. Film-forming ability of PCL/XG/CSP composites prepared with different emulsifiers

Table 2 presents the film-forming ability of PCL/XG/CSP composites prepared with different auxiliary agents including PEO, PEG, Tween 80, and Tween 20. It can be seen that when using the Tween 80 or Tween 20, the PCL/XG/CSP composites cannot form a film, the samples don't dry naturally or after drying in an oven. Similar to using PEG, the composites also don't dry naturally but they become dry after 72 hours of drying at 80 °C. However, the color of the samples changes from yellow to light pink due to the CSP conversion. Additionally, the CSP was agglomerated to each other in the composite films. In contrast, when the addition of PEO, the PCL/XG/CSP composites are easily formed in a film form with a smooth surface. In the case of the absence of PEO, the PCL/XG/CSP composites have film-forming ability but the obtained films are less uniform due to the existence of CSP clusters in the samples. From that, it can be recognized that among investigated auxiliary agents, PEO is the most suitable auxiliary agent for the preparation of the PCL/XG/CSP composite films with a homogeneous structure. This result is in agreement with other reports [21, 22]. The ether oxygen and terminal hydroxyl groups in PEO can form a hydrogen bond with the hydroxyl and ether groups in PCL, XG, and CSP [22].

In this study, the weight ratio of PCL/XG in the PCL/XG/CSP composite films was also studied. The samples with higher content of XG tend to form the film better than those with lower content of XG. When using a high XG content, it requires a longer time for drying PCL/XG/CSP composite films. Therefore, a PCL/XG ratio of 70/30 has been selected for further studies.

The amount of PEO in the PCL/XG/CSP composites was varied by 0.6 g, 0.4 g, 0.2 g, 0.1 g, and 0.05 g. In the case of using low PEO content, the samples XPC37PEO1 and XPC37PEO0.5 exhibit the film-forming ability but CSP tends to aggregate in the composite films. When increasing PEO content to 0.4 g, the PCL/XG/CSP composites can be formed in the film form, however, the agglomeration of CSP is still observed. In contrast, using 0.6 g of PEO can help to obtain a regular film. Therefore, 0.6 g of PEO is the suitable content for the preparation of PCL/XG/CSP composite films.

When using the same volume of solvents, the concentration of polymers in the solution can influence on the properties of the PCL/XG/CSP composite films. It can be seen the concentration of PCL and XG in the solution does not affect the film-forming ability of the PCL/XG/CSP composite films. The obtained composite films have even and smooth surfaces. It is required further assessment to find the suitable concentration of polymers in the solution.

Table 2. The film-forming ability of PCL/XG/CSP composites prepared with different emulsifiers.

No.	Sample	Film-forming ability
1	XPC46	Have the film-forming ability, CSP agglomeration
2	XPC46PEO6	Have the film-forming ability, smooth surface
3	XPC46PEG6	Have the film-forming ability
4	XPC46Tween806	Cannot form a film
5	XPC46Tween206	Cannot form a film
6	XPC37	Have the film-forming ability, CSP agglomeration
7	XPC37PEO6	Have the film-forming ability, smooth surface
8	XPC37PEG6	Have the film-forming ability
9	XPC37Tween806	Cannot form a film
10	XPC37Tween206	Cannot form a film
11	XPC28	Have the film-forming ability, CSP agglomeration
12	XPC28PEO6	Have the film-forming ability, smooth surface
13	XPC28PEG6	Have the film-forming ability
14	XPC28Tween806	Cannot form a film
15	XPC28Tween206	Cannot form a film
16	XPC19	Have the film-forming ability, CSP agglomeration
17	XPC19PEO6	Have the film-forming ability
18	XPC19PEG6	Have the film-forming ability
19	XPC19Tween806	Cannot form a film
20	XPC19Tween206	Cannot form a film
21	XPC37PEO4	Have the film-forming ability, smooth surface, CSP agglomeration
22	XPC37PEO2	Have the film-forming ability, CSP agglomeration
23	XPC37PEO1	Have the film-forming ability, CSP agglomeration
24	XPC37PEO0.5	Have the film-forming ability, CSP agglomeration
25	XPC614PEO6	Have the film-forming ability, smooth surface
26	XPC921PEO6	Have the film-forming ability, smooth surface
27	XPC1228PEO6	Have the film-forming ability, smooth surface

3.2. FT-IR spectra of PCL/XG/CSP composites prepared with the suitable emulsifier

In our previous study, the FT-IR spectra of PCL, XG, and CSP have been presented [24]. In which, the PCL exhibits the vibrations of C-H (2923 cm^{-1} and 2863 cm^{-1}), C=O (1724 cm^{-1}), C-O and C-C (1050 – 1290 cm^{-1}) bonds; the XG exhibits the vibrations of O-H (3284 cm^{-1} and 1600 cm^{-1}), C-H (2919 cm^{-1}, 1406 cm^{-1}), C=O (1726 cm^{-1}), C-O, C-C (1020-1250 cm^{-1}) bonds; the CSP exhibits the vibrations of C=O and C=C (1728 cm^{-1} and 1675 cm^{-1}), C-O and C-C (1024-1266 cm^{-1}) bonds [24].

The FI-IR spectra of PCL/XG/CSP composite samples prepared with different auxiliary agents and a fixed PCL/XG ratio of 70/30 have been reported in Figure 1 as representative samples. It can be seen the vibrations characterized for the main functional groups of PCL, XG, and CSP appeared in the FT-IR spectra of the composite samples. XG/PCL sample only exhibits the vibrations of the ester group at 1721, 1241, and 1044 cm^{-1}, without C=C vibration [24]. The stretching vibration of C=C linkage of CSP at 1600 cm^{-1} was found in the FT-IR spectra of the PCL/XG/CSP composite samples prepared with different auxiliary agents and fixed PCL/XG ratio of 70/30, suggesting that CSP has been included in the PCL/XG polymer matrix. In the case of using auxiliary agents, the absorbance peaks characterized for the vibrations of C-H bonds are sharp and have higher intensity compared to sample XPC37 without ones. This is evidence for the existence of auxiliary agents in the PCL/XG/CSP composite samples. A slight shift in wavenumbers of characteristic peaks in the FT-IR spectra of the composite samples in comparison to the FT-IR spectra of PCL, XG, or CSP, suggesting that the PCL, XG, and CSP can interact with each other in the presence of auxiliary agents. The difference in the peak at 2360 cm^{-1} between sample spectra may be caused by the noise signal of CO_2 in the air.

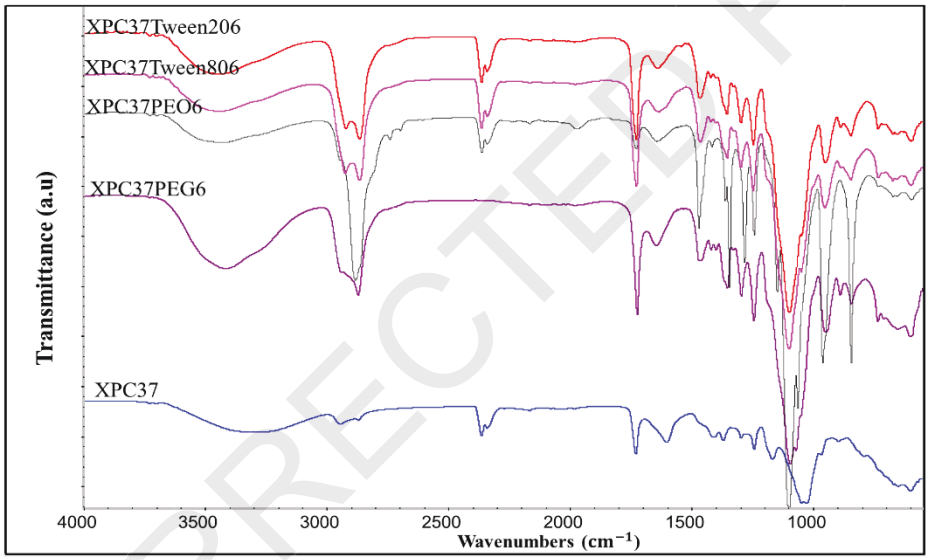

Figure 1. FI-IR spectra of PCL/XG/CSP composite samples prepared with different auxiliary agents and fixed PCL/XG ratio of 70/30.

The FT-IR spectra of PCL/XG/CSP composite samples prepared with different conditions (different PCL/XG ratios, different PEO contents, and different PCL and XG concentrations) are presented in the supplement file. It can be seen that the change in composition ratios of the PCL/XG/CSP composite does not influence the vibrations of the main function groups in the composite films. Thus, it requires the assessment of the morphology of the composite samples to give detailed comments on the effect of preparation conditions on the film-forming ability of the PCL/XG/CSP composites.

3.3. Morphology of PCL/XG/CSP composites prepared with the suitable auxiliary agent

The stereo-microscopy (SM) images of the PCL/XG/CSP composites without auxiliary agents are revealed in Figure 2. It can be seen that the composites have an uneven structure with

the yellow clusters of CSP and PCL in the XG matrix. Therefore, using auxiliary agents is necessary to enhance the dispersibility of PCL and CSP in the XG matrix.

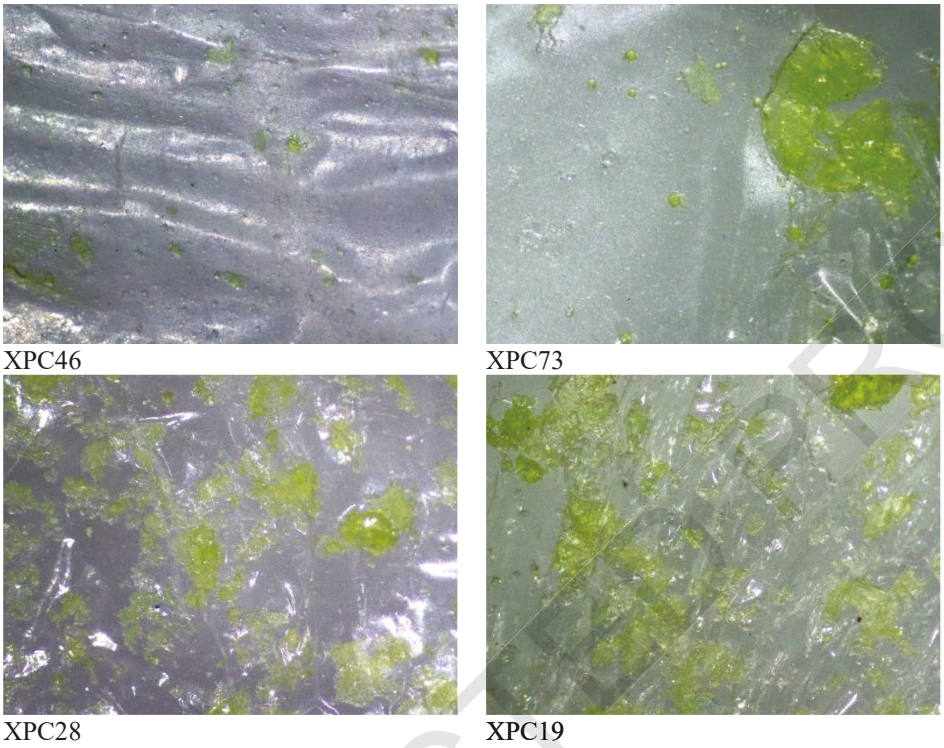

Figure 2. SM images of the PCL/XG/CSP composites.

Figure 3 displays the SM images of the PCL/XG/CSP composite films prepared with different PCL/XG ratios and a fixed PEO content of 0.6 g. Samples XPC19PEO6 and XPC46PEO6 have an irregular structure, in which the PCL/CSP dispersion phase was spherical and there are air bubbles appeared in the films. Samples XPC28PEO6 and XPC37PEO6 exhibit a very regular structure with a good mix of components. Among investigated samples, the dispersion of CSP in the sample XPC37PEO6 is the best. Therefore, the PCL/XG ratio of 70/30 is the most suitable for the preparation of PCL/XG/CSP/PEO composite films.

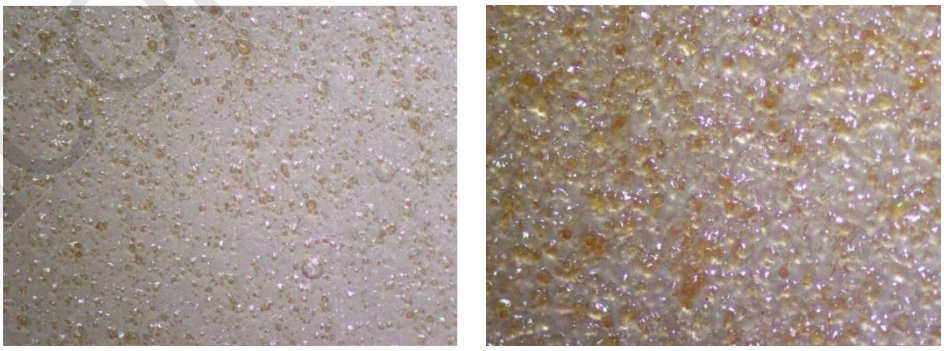

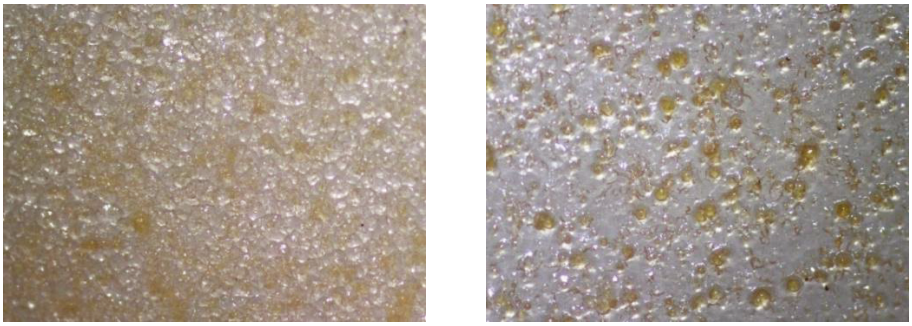

XPC28PEO6 XPC19PEO6

Figure 3. SM images of the PCL/XG/CSP/PEO composites prepared with different PCL/XG ratios.

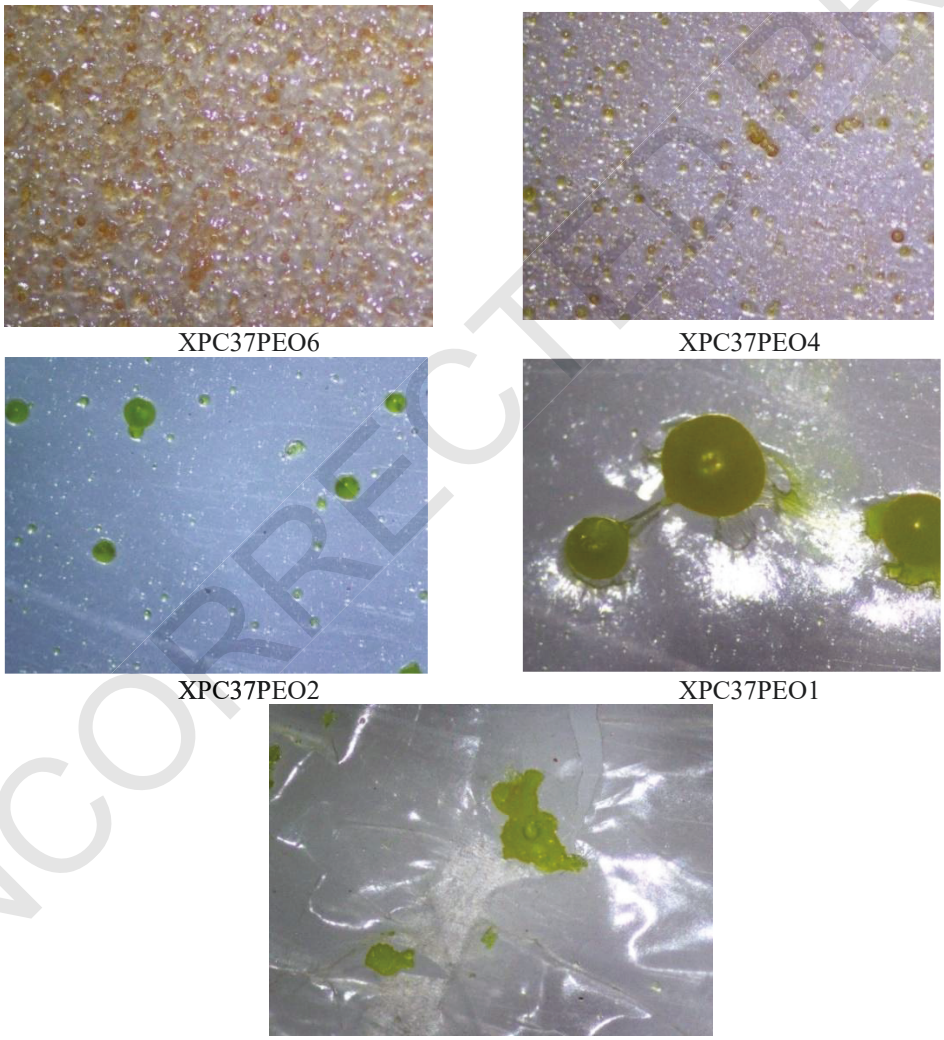

XPC37PEO6 XPC37PEO4

XPC37PEO2 XPC37PEO1

XPC37PEO0.5

Figure 4. SM images of the PCL/XG/CSP/PEO composite films prepared with different PEO contents.

The SM images of the PCL/XG/CSP/PEO composite films prepared with different PEO contents in Figure 4 indicate that the sample XPC37PEO6 has the best even structure while the others contain PCL/CSP clusters. This is evidence of the poor dispersibility of PCL/CSP in the XG matrix in the case of using a low PEO emulsifier content. Therefore, 0.6 g of PEO has been selected for the preparation of PCL/XG/CSP/PEO composite films.

Figure 5 performs the SM images of the PCL/XG/CSP/PEO composites prepared with different PCL and XG concentrations. It can be seen that when increasing the weight of PCL and XG in the samples, the structure of the composite films becomes uneven. The XPC37PEO6 and XPC614PEO6 samples have a regular structure with a great dispersion of PCL and CSP in the XG matrix.

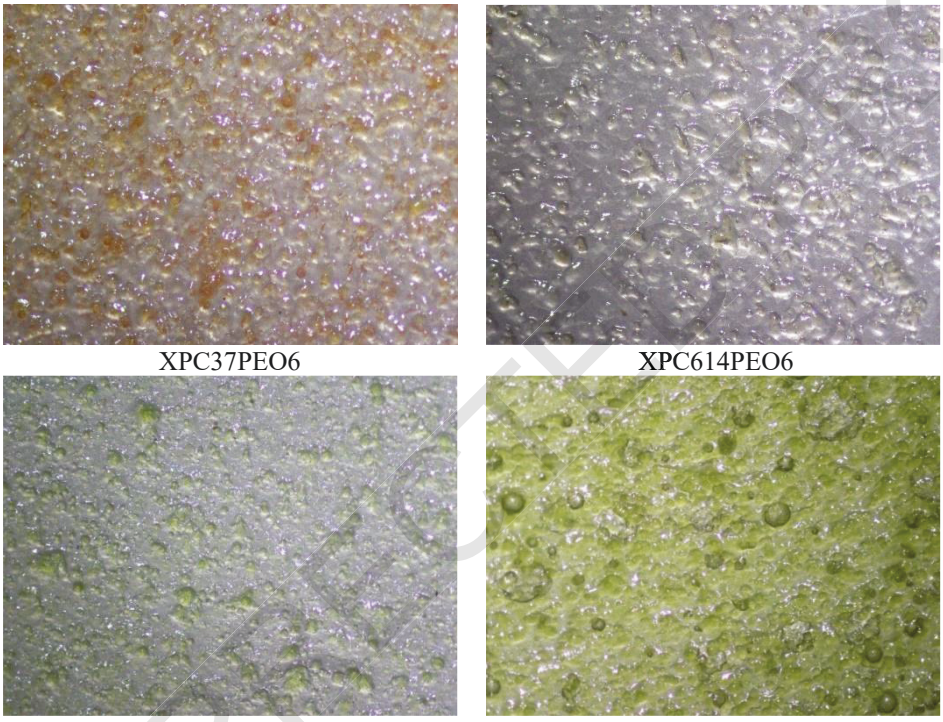

Figure 5. SM images of the PCL/XG/CSP/PEO composite films prepared with different PCL and XG concentrations.

3.4. Mechanical properties of PCL/XG/CSP composites prepared with the suitable emulsifier

For opening the application capacity of the PCL/XG/CSP/PEO composite films in practice, their mechanical property is one of the important parameters [15, 25, 26]. Table 3 displays the tensile strength and elongation at break of the PCL/XG/CSP/PEO composite films. The tensile strength and elongation at break of the PCL/XG/CSP/PEO composite films have been improved in the presence of XG. The combination of XG and PCL can enhance the durability of samples with the formation under the impact of the external force. The PCL/XG ratios have a strong effect on the mechanical properties of the PCL/XG/CSP/PEO composite films. Among investigated samples, the XPC37PEO6 sample has the highest tensile strength and elongation at

break, reaching 4.55 MPa and 11.12 %, respectively. This is thanks to the even dispersion of CSP and PCL in the XG matrix, leading to the limitations of stress at the point of clusters.

The elongation at break of the XPC37PEO6 sample is higher than that of the XPC37PEO4 sample while its tensile strength follows an opposite trend. Combined with SM images as above mentioned, PEO 0.6 g has been still chosen for the preparation of PCL/XG/CSP/PEO composite films.

When increasing the PCL and XG concentration in the composite samples up a moderate amount, the tensile strength and elongation at break of the composite films have been enhanced. For instance, the tensile strength of sample XPC614PEO6 is 8.81 MPa while its elongation at break is 13.05 %. However, if the content of PCL and XG in the sample is higher, the elongation at break is reduced slightly but the tensile strength of the composites is declined sharply. This is due to the agglomeration of PCL and CSP in the samples, leading to the appearance of defects, that concentrated stress in the break process.

From the obtained results, the most suitable conditions for the preparation of sample XPC614PEO6 composite film are a PCL/XG ratio of 70/30, PEO content of 0.6 g, PCL concentration of 0.14 g/2 mL DCM, and XG concentration of 0.06 g/10 mL distilled water.

Table 3. Mechanical properties of the PCL/XG/CSP/PEO composite films.

No.	Sample	Tensile strength (MPa)	Elongation at break (%)
1	XPC46PEO6	2.02 ± 0.80	8.30 ± 2.22
2	XPC37PEO6	4.55 ± 0.54	11.12 ± 1.9
3	XPC28PEO6	3.81 ± 0.78	4.24 ± 0.55
4	XPC19PEO6	6.16 ± 0.74	5.78 ± 0.79
5	XPC37PEO4	6.00 ± 0.56	7.71 ± 0.56
6	XPC614PEO6	8.81 ± 0.79	13.05 ± 1.35
7	XPC921PEO6	1.88 ± 0.03	11.12 ± 0.58
8	XPC1228PEO6	2.58 ± 0.53	8.88 ± 0.28
9	PCL/CSP/PEO6	2.22 ± 0.55	4.73 ± 0.93

3.5. Some characteristics of PCL/XG/CSP composite film prepared with the most suitable conditions

The SEM images of the XPC614PEO6 sample at the magnification of 500 and 20000 times in Figure 6 indicate a heterogenous structure of the composite film. The CSP/PCL is the dispersion phase while XG/PEO is the continuous phase. The size of the dispersion phase ranged from 4-10 μm. The spherical CSP/PCL particles were dispersed evenly on the XG/PEO matrix. At higher magnification, the compositions in the composites can be mixed well without cracks or defects. The even structure is one of the advantages of the PCL/XG/CSP composite prepared with the most suitable conditions, which leads to improvement in the tensile strength and elongation at break as above mentioned.

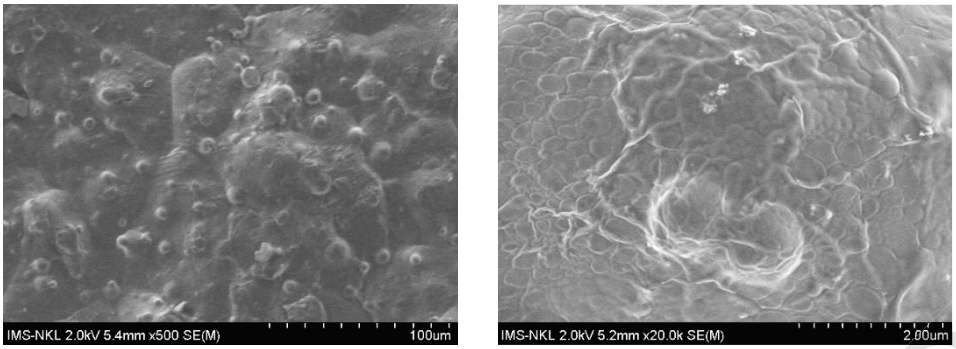

Figure 6. SEM images of XPC614PEO6 composite film.

Figure 7 demonstrates the DSC diagrams of PCL, XG, CSP, PEO, and XPC614PEO6 composite film. In our previous study, the DSC diagram of CSP exhibited an endothermic peak at 196.9 °C corresponding to the melting temperature of CSP crystals while that of PCL exhibited a sharp peak at 70.6 °C corresponding to the melting point of PCL [27]. The DSC diagram of XG indicates a broad peak at 76.0 °C that is characterized by the melting process of XG [28, 29]. The DSC diagram of PEO also shows a sharp peak at 69.3 °C, assigned to the melting temperature of PEO [30]. The DSC diagram of sample XPC614PEO6 exhibits only one sharp endothermic peak at 71.4 °C with a melting enthalpy of 160.5 J/g. Moreover, the width of this peak is larger than that of peaks of PCL or PEO, showing the interaction of components in the composite film. This suggests that the PCL, XG, PEO, and CSP are well-compatible with each other [31, 32]. Moreover, one glass transition is also observed at a mid-temperature of 248.2 °C that characterized for glass transition of CSP with a delta C_p of 1.479 J/(gK). This is evidence for the incorporation of CSP in the composite structure. It can not observe the melting peak of CSP at 196.9 °C [24, 31], suggesting that the crystal degree of CSP is reduced when combined with PCL and XG in the composite.

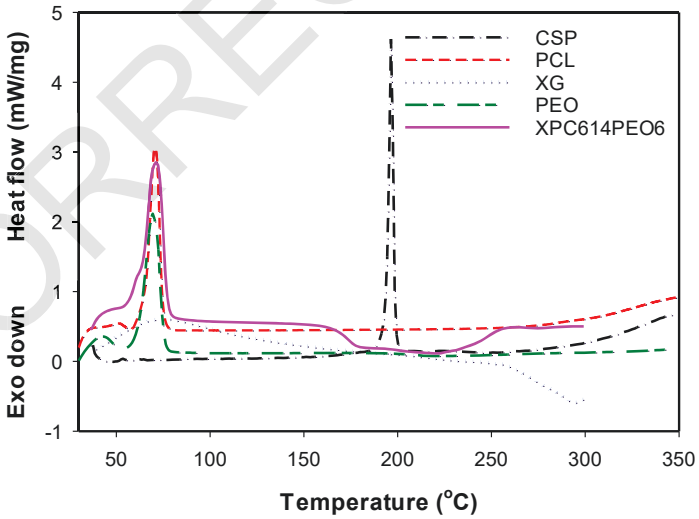

Figure 7. DSC diagrams of PCL, XG, CSP, PEO, and XPC614PEO6 composite film.

The XRD pattern of the XPC614PEO6 sample is shown in Figure 8. The PCL still exhibits the semi-crystal structure with two main diffraction peaks at 2θ of approximately 21.4° and 24.3°, assigned to (110) and (201) plans, respectively [32]. It can be seen the absence of crystal

peaks of CSP at 2θ of 8.294° and 16.287° [31], suggests the reduction in the crystal degree of CSP in the composite. This reduction indicates the amorphous state of CSP in the composite [31, 33], benefiting for drug release process in simulated human body fluids.

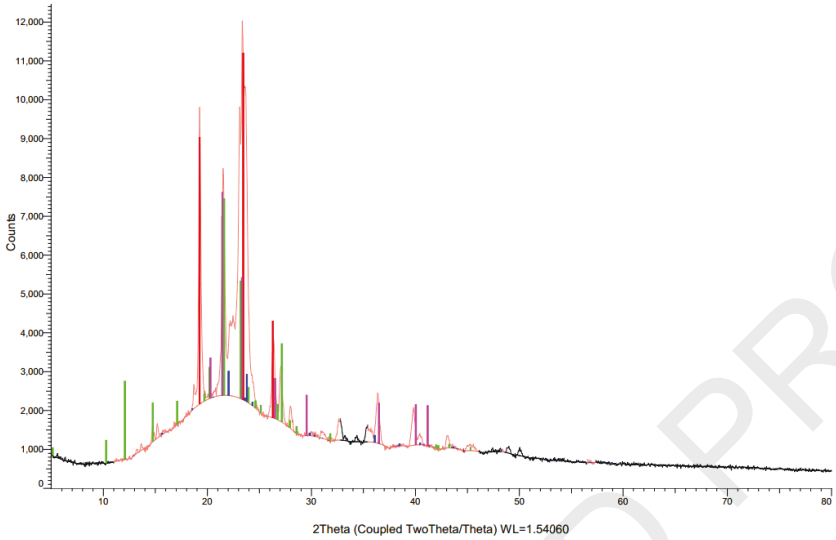

Figure 8. XRD pattern of XPC614PEO6 composite film.

WCA is one of the important parameters contributing to the surface properties of composite film materials. When the film has a WCA less than 90°, it shows that the film is hydrophilic while a WCA greater than 90° exhibits a hydrophobic property. The image of the water droplet in Figure 9 indicates that the surface of the XPC614PEO6 composite film is hydrophilic, with a WCA value of 45.5°. This is one advantage of the contact of the film with water molecules in the testing environments.

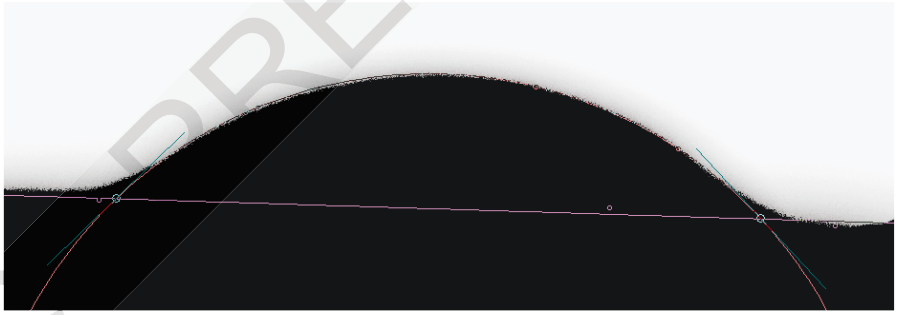

Figure 9. Image of the water droplet on the surface of sample XPC614PEO6.

4. CONCLUSION

In this study, the auxiliary agents including PEO, PEG, Tween 80, and Tween 20 have a strong effect on the film-forming ability of the PCL/XG/CSP composites that were prepared by the solution casting method. The PEO is the most suitable agent for the preparation of the PCL/XG/CSP composites with great film-forming ability and the obtained films having smooth and even surfaces. The PEO content, PCL/XG ratio, and PCL and XG concentration influenced strongly on the morphology and mechanical properties of the PCL/XG/CSP/PEO composite

films while they did not affect the functional groups in the structure of the composites. The PEO content of 0.6 g, the PCL/XG of 70/30, and the PCL and XG contents of 0.14 and 0.06 g, respectively, are the most suitable ratios for the preparation of the even PCL/XG/CSP/PEO composite films. The PCL/CSP dispersion phase in spherical shape with a size of 4-10 µm is dispersed regularly in the XG/PEO matrix. The crystal degree of CSP reduced significantly in combination with PCL, XG, and PEO. The PCL/XG/CSP/PEO composite film prepared at the most suitable conditions has a hydrophilic surface, benefiting from the contact of the film with water molecules in the simulated body fluids. It is required to do more experiments to assess the characteristics and properties, drug loading capacity, drug release content, drug release kinetic, and bioactivities of the PCL/XG/CSP/PEO composite films prepared at the most suitable conditions to develop the potential applications of these composite films in practice.

Acknowledgment. This research is funded by Vietnam National Foundation for Science and Technology Development (NAFOSTED) under grant number 104.02-2021.48.

CRediT authorship contribution statement. Nguyen Thuy Chinh: Investigation, Formal analysis, Writing – original draft. Trinh Hoang Nghia, Pham Thi Huyen: Investigation. Thai Hoang: Conceptualization, Supervision, Funding acquisition, Writing – review & editing.

Declaration of competing interest. The authors declare that they have no known competing financial interests or personal relationships that could have appeared to influence the work reported in this paper.

REFERENCES

1. Shaikh A. A., Datta P., Dastidar P., Majumder A., Das M. D., Manna P., Roy S. - Biopolymer-based nanocomposites for application in biomedicine: a review. J. Polym. Eng., **44**(2) (2024) 83-116. https://doi.org/10.1515/polyeng-2023-0166.
2. Beach M. A., Nayanathara U., Gao Y., Zhang C., Xiong Y., Wang Y., Such G. K. - Polymeric nanoparticles for drug delivery. Chem. Rev., **124**(9) (2024) 5505-5616. https://doi.org/10.1021/acs.chemrev.3c00705.
3. Nguyen T. C., Thai H. - Review: fish collagen: extraction, characterization and application in wound healing and drug delivery. Vietnam J. Sci. Technol., **62**(1) (2024) 1-22. https://doi.org/10.15625/2525-2518/19438.
4. Nasiri S. S., Ahmadi Z., Afshar-Taromi F. - Synthesis Biomaterials in Biomedical Applications. In *Functional Biomaterials*, Springer, Singapore (2022) 285-317.
5. Ananth K. P., Jayram N. D. - A comprehensive review of 3D printing techniques for biomaterial-based scaffold fabrication in bone tissue engineering. Ann. 3D Print. Med., **13** (2024) 100141. https://doi.org/10.1016/j.stlm.2023.100141.
6. Algharib S. A., Dawood A., Zhou K., Chen D., Li C., Meng K., Zhang A., Luo W., Ahmed S., Huang L., Xie S. - Preparation of chitosan nanoparticles by ionotropic gelation technique: Effects of formulation parameters and in vitro characterization. J. Mol. Struct., **1252** (2022) 132129. https://doi.org/10.1016/j.molstruc.2021.132129.
7. Nguyen T. C., Thai H. - Review: Emulsion techniques for producing polymer based drug delivery systems. Vietnam J. Sci. Technol., **61**(1) (2023) 1-26. https://doi.org/10.15625/2525-2518/17666.
8. Dawin T. P., Ahmadi Z., Taromi F. - Bio-based solution-cast blend films based on polylactic acid and polyhydroxybutyrate: influence of pyromellitic dianhydride as chain extender on the morphology, dispersibility, and crystallinity. Prog. Org. Coat., **119** (2018) 23-30. https://doi.org/10.1016/j.porgcoat.2018.02.003.
9. Wu C., Peng S., Wen C., Wang X., Fan L., Deng R., Pang J. - Structural characterization and properties of konjac glucomannan/curdlan blend films. Carbohydr. Polym., **89**(2) (2012) 497-503. https://doi.org/10.1016/j.carbpol.2012.03.034.

10. Notario-Pérez F., Cazorla-Luna R., Martín-Illana A., Galante J., Ruiz-Caro R., das Neves J., Veiga M. D. - Design, fabrication and characterisation of drug-loaded vaginal films: State-of-the-art. J. Control. Release, **327** (2020) 477-499. https://doi.org/10.1016/j.jconrel.2020.08.032.
11. Dwivedi R., Kumar S., Pandey R., Mahajan A., Nandana D., Katti D. S., Mehrotra D. - Polycaprolactone as biomaterial for bone scaffolds: Review of literature. J. Oral Biol. Craniofac. Res., **10**(1) (2020) 381-388. https://doi.org/10.1016/j.jobcr.2019.10.003.
12. Kirmanidou Y., Chatzinikolaidou M., Michalakis K., Tsouknidas A. - Clinical translation of polycaprolactone-based tissue engineering scaffolds, fabricated via additive manufacturing: A review of their craniofacial applications. Biomater. Adv., **162** (2024) 213902. https://doi.org/10.1016/j.bioadv.2024.213902.
13. Yang Y., Wu H., Fu Q., Xie X., Song Y., Xu M., Li J. - 3D-printed polycaprolactone-chitosan based drug delivery implants for personalized administration. Mater. Des., **214** (2022) 110394. https://doi.org/10.1016/j.matdes.2022.110394.
14. Schlesinger E., Ciaccio N., Desai T. A. - Polycaprolactone thin-film drug delivery systems: Empirical and predictive models for device design. Mater. Sci. Eng. C, **57** (2015) 232-239. https://doi.org/10.1016/j.msec.2015.07.027.
15. Herrera N., Olsén P., Berglund L. A. - Strongly improved mechanical properties of thermoplastic biocomposites by PCL grafting inside holocellulose wood fibers. ACS Sustain. Chem. Eng., **8**(32) (2020) 11977-11985. https://doi.org/10.1021/acssuschemeng.0c02512.
16. Malik N. S., Ahmad M., Minhas M. U., Tulain R., Barkat K., Khalid I., Khalid Q. - Chitosan/Xanthan gum based hydrogels as potential carrier for an antiviral drug: fabrication, characterization and safety evaluation. Front. Chem., **8** (2020) 50. https://doi.org/10.3389/fchem.2020.00050.
17. Hajikhani M., Khanghahi M. M., Shahrousvand M., Mohammadi-Rovshandeh J., Babaei A., Khademi S. M. H. - Intelligent superabsorbents based on a xanthan gum/poly (acrylic acid) semi-interpenetrating polymer network for application in drug delivery systems. Int. J. Biol. Macromol., **139** (2019) 509-520. https://doi.org/10.1016/j.ijbiomac.2019.07.221.
18. Xie L., Tang H., Song J., Long J., Zhang L., Li X. - Chrysophanol: a review of its pharmacology, toxicity and pharmacokinetics. J. Pharm. Pharmacol., **71**(10) (2019) 1475-1487. https://doi.org/10.1111/jphp.13143.
19. Prateeksha, Yusuf M. A., Singh B. N., Sudheer S., Kharwar R. N., Siddiqui S., Abdel-Azeem A. M., Fernandes Fraceto L., Dashora K., Gupta V. K. - Chrysophanol: A natural anthraquinone with multifaceted biotherapeutic potential. Biomolecules, **9**(2) (2019) 68. https://doi.org/10.3390/biom9020068.
20. Su S., Wu J., Gao Y., Luo Y., Yang D., Wang P. - The pharmacological properties of chrysophanol, the recent advances. Biomed. Pharmacother., **125** (2020) 110002. https://doi.org/10.1016/j.biopha.2020.110002.
21. da Rosa C. G., Sganzerla W. G., de Oliveira Brisola Maciel M. V., de Melo A. P. Z., da Rosa Almeida A., Ramos Nunes M., Bertoldi F. C., Manique Barreto P. L. - Development of poly (ethylene oxide) bioactive nanocomposite films functionalized with zein nanoparticles. Colloids Surf. A: Physicochem. Eng. Asp., **586** (2020) 124268. https://doi.org/10.1016/j.colsurfa.2019.124268.
22. Çaykara T., Demirci S., Eroğlu M. S., Güven O. - Poly(ethylene oxide) and its blends with sodium alginate. Polymer, **46**(24) (2005) 10750-10757. https://doi.org/10.1016/j.polymer.2005.09.041.
23. Gu Y., Pang Y., Yang D., Qian Y., Lou H., Zhou M. - Preparation of lignin/polyethylene glycol film-forming agent and its application in chlorantraniliprole 5% flowable concentrate for seed coating (FS). Ind. Crops Prod., **182** (2022) 114877. https://doi.org/10.1016/j.indcrop.2022.114877.
24. Vu T. T. L., Nguyen T. C., Duong T. M., Tran D. T., Pham T. H. T., Tran T. M., Ly T. N. L., Thai H. - Chrysophanol-loaded composites with xanthan gum/polycaprolactone for drug release enhancement. ChemistrySelect, **9**(34) (2024) e202402196. https://doi.org/10.1002/slct.202402196.
25. Dilkushi H. A. S., Jayarathna S., Manipura A., Chamara H. K. B. S., Edirisinghe D., Vidanarachchi J. K., Priyashantha H. - Development and characterization of biocomposite films using banana

pseudostem, cassava starch and poly(vinyl alcohol): A sustainable packaging alternative. Carbohydr. Polym. Technol. Appl., **7** (2024) 100472. https://doi.org/10.1016/j.carpta.2024.100472.

26. Hashim H. b., Emran N. A. A. b., Isono T., Katsuhara S., Ninoyu H., Matsushima T., Yamamoto T., Borsali R., Satoh T., Tajima K. - Improving the mechanical properties of polycaprolactone using functionalized nanofibrillated bacterial cellulose with high dispersibility and long fiber length as a reinforcement material. Compos. Part A: Appl. Sci. Manuf., **158** (2022) 106978. https://doi.org/10.1016/j.compositesa.2022.106978.
27. Nguyen T. C., Trinh H. N., Do T. M., Ly T. N. L., Thai H. - Preparation and characterization of biomaterials based on polycaprolactone and chrysophanol. Vietnam J. Sci. Technol., (2024) In press.
28. Yang Q., Li Y., Cao Z., Miao J., Feng J., Xi Q., Lu W. - Structure-property relationship in the evaluation of xanthan gum functionality for oral suspensions and tablets. Int. J. Biol. Macromol., **226** (2023) 525-534. https://doi.org/10.1016/j.ijbiomac.2022.12.081.
29. Tegopoulos S. N., Papagiannopoulos A., Kyritsis A. - Hydration effects on thermal transitions and molecular mobility in Xanthan gum polysaccharides. Phys. Chem. Chem. Phys., **26**(4) (2024) 3462-3473. https://doi.org/10.1039/D3CP04643E.
30. Caramia V., Bayer I. S., Anyfantis G. C., Ruffilli R., Ayadi F., Martiradonna L., Cingolani R., Athanassiou A. - Tailoring the morphology of poly(ethylene oxide)/silver triflate blends: from crystalline to self-assembled nanofibrillar structures. Nanotechnology, **24**(5) (2013) 055602. https://doi.org/10.1088/0957-4484/24/5/055602.
31. Devendra S., Rawat M. S. M., Ajay S., Mona S. - Chrysophanol-phospholipid complex. A drug delivery strategy in herbal novel drug delivery system (HNDDS). J. Therm. Anal. Calorim., **111** (2013) 2069-2077.
32. Domínguez-Robles J., Cuartas-Gómez E., Dynes S., Utomo E., Anjani Q. K., Detamornrat U., Donnelly R. F., Moreno-Castellanos N., Larrañeta E. - Poly(caprolactone)/lignin-based 3D-printed dressings loaded with a novel combination of bioactive agents for wound-healing applications. Sustain. Mater. Technol., **35** (2023) e00581. https://doi.org/10.1016/j.susmat.2023.e00581.
33. Bruni G., Milanese C., Berbenni V., Sartor F., Villa M., Marini A. - Crystalline and amorphous phases of a new drug. J. Therm. Anal. Calorim., **102** (2009) 297-303. https://doi.org/10.1007/s10973-009-0614-2.